ANTICANCER RESEARCH *24*: 1689-1698 (2004)

A Simple Model to Simulate Cellular Changes in the T Cell System Following HIV-1 Infection

GUANYU WANG[1,3], GERHARD R. F. KRUEGER[2] and L. MAXIMILIAN BUJA[1]

[1]*Department of Pathology & Laboratory Medicine and* [2]*Department of Internal Medicine, University of Texas - Houston Medical School, Houston, Texas 77030;*
[3]*Center for Computational Biomedicine, School of Health Information Sciences, University of Texas Health Sciences Center, Houston, Texas 77030, U.S.A.*

Abstract. *A new mathematical model is presented to simulate various changes of cell pools in the T cell immune system with validation procedures imitating viral infections. The present paper focuses on changes during the course of an acute progressive HIV-1 infection. Parameters are optimized by a direct search method and the stability of the model is studied. Mathematical modeling supports the hypothesis that the differentiation blockade is one major reason for the depletion of CD4 cells and the proliferation of CD38 cells in HIV-1 infection. The model appears to be a useful basis for further simulating disturbances of the T cell immune system in other viral infections as well as to elucidate the pathogenesis of various immunological diseases including the development of malignant lymphomas.*

In recent years, many mathematical models have been developed to describe the immunological response to infection with human immunodeficiency virus (HIV) (*e.g.*, Nowak & May, 1991; Nowak & Bangham, 1996; Perelson *et al.*, 1993 & 1996; Essunger & Perelson, 1994; Kirschner *et al.*, 1998; Kirschner *et al.*, 2000; Mehr & Perelson, 1997; Culshaw & Ruan, 2000). Some important parameters, such as the virion clearance rate, the infected cell life-span and the average viral generation time were estimated fairly well by these models. However, this pertains only to the initial stage of the infection (with a time scale in days), in which case one needs only to consider the interaction between the CD4 T cells and the virus. Although some of these models are supported by clinical data, the data appear to be abstracted and no further information is available about the case material from which such data were obtained (Krueger *et al.*, 2001a). In addition, these data were obtained from the patients with the administration of protease/reverse-transcriptase inhibitors. We are focusing, instead, on the natural course of HIV infection with data from patients before antiviral treatment was established.

To model HIV dynamics of the entire infectious course (*i.e.*, from infection to the death of the incumbent), different T cell pools in the immune system should be studied in order to consider eventual reparatory cell changes. The course of the T cell development runs from the undifferentiated stem cell pool through various developmental stages to mature cells. The process is under critical control of the thymic microenvironment including such components as reticular epithelial cells, macrophages and fibroblasts (Stutman, 1978; Atkins *et al.*, 1987; Lobach & Haynes, 1987; Dappen *et al.*, 1982; Surh & Sprent, 1999; Abramson *et al.*, 1977; Thiele *et al.*, 1995). Such microenvironmental cells which influence the proliferation and maturation of T lymphocytes by various secretory products are unequally distributed in the thymus separating this organ into several poorly defined compartments (Heine *et al.*, 1983; Atkins *et al.*, 1987; Crouse *et al.*, 1980; Rothenberg & Lugo, 1985; Wognum *et al.*, 1996; Marrack *et al.*, 1988; Peled *et al.*, 1999). Consequently, T cell differentiation can be divided into several phases: the prethymic phase, thymic cortical phase, thymic medullary phase and the postthymic phase. In each phase, T lymphocytes of different phenotypes can be identified, although the transition from one phase to the other is rather fluent. In addition, T cell antigen receptor rearrangements identify various stages of cell maturation (Stutman, 1978; Allison, 1987; Miescher *et al.*, 1988, Kronenberg *et al.*, 1986). A simplified block diagram of T cell maturation is shown in Figure 1 with individual T cell pools identified by selective CD markers. To reduce complexity, in the present study we do not simulate the thymic medullary (CD4+8+) cells.

Correspondence to: Guanyu Wang, Ph.D., Department of Pathology and Laboratory Medicine, University of Texas-Houston Medical School, 6431 Fannin, Houston, TX 77030, U.S.A. Tel: (713) 500-6060, Fax: (713) 500-0730, e-mail: Guanyu.Wang@uth.tmc.edu

Key Words: Immune system modeling, HIV infection, delay differential equation.

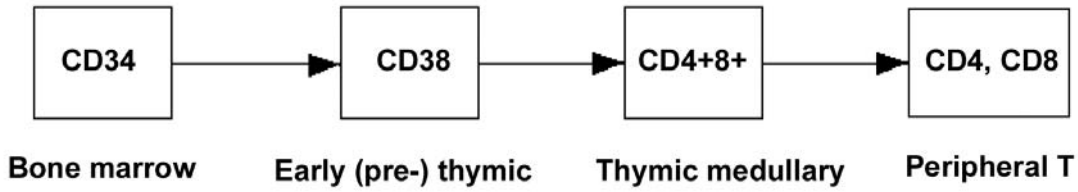

Figure 1. *The simplified block diagram of T cell maturation.*

Figure 2 shows the block diagram of the infectious process. The output from the CD34 cell pool, namely the source for the CD38 T cells *(Z)* is assumed to be constant. CD38 T cells differentiate into CD4 cells and CD8 cells *(Y)* under the control of thymopoietins that are produced by the thymic epithelial cells. The thymic epithelial cells can be killed by HIV-1 virus *(V)*, which blocks the differentiation and consequently leads to the proliferation of CD38 cells and the decreases of CD4 and CD8 cells (Seemayer *et al.*, 1984; Purtilo *et al.*, 1985; Kendall, 1986; Bonyhadi *et al.*, 1993; Braun *et al.*, 1996; Haynes *et al.*, 1998; Krueger *et al.*, 2001a). Similar to others (*e.g.*, Culshaw & Ruan, 2000), we split the CD4 T cells into two subgroups: the (virus) infected CD4 cells *(T_i)* and uninfected CD4 cells *(T)*. To reduce complexity, we did not further split T_i into the latently infected cells and the productively infected cells, like Perelson *et al.* (1993). The CD4 T cells are the major target of HIV-1. After the binding of HIV-1 to the cellular CD4 receptor, the virus fuses with the cytoplasmic membrane, becomes rapidly internalized within a few minutes and uncoated (Sinangil *et al.*, 1988). While virus replicates, the infected CD4 cells become antigenic and stimulate the proliferation of the CD8 T cells, which in turn kill the infected CD4 T cells. Besides this, the infected CD4 T cells die in response to the virus replication.

Data Acquisition

Data for validating our computer simulation are taken from several clinical studies including a randomized double-blind study of administering immunoglobulins to HIV infected persons (Krueger *et al.*, 1990 & 2001a; Tymister, 1988; Kirn *et al.*, 1993). A total of 200 HIV-1-positive patients were followed at the Immunopathology Laboratory, University of Cologne, Germany, between 1983 and 1990. HIV infection was proven by two independent positive HIV-1 antibody ELISA tests and further confirmed by showing cytopathic effects and virial antigen expression by indirect immunofluorescence in tissue culture cells, as well as by Western blot (Organon Teknika, Turnhout, Belgium; Abbott Laboratories, Wiesbaden, Germany). Nineteen of these patients were selected for our present study according to the following criteria: a) all patients had signs of an acute syndrome (Table I, Fauci & Clifton, 2001) supporting tentative timing of the infection; b) disease progression from HIV positivity and stage WR1 or WR2 to stage WR6 (Redfield *et al.*, 1986) within 5 years; c) complete clinical follow-up at Cologne University Clinics for Dermatology (Prof. Dr. G. K. Steigleder) of Medicine II (Prof. Dr. W. Kaufmann); d) availability of liquid-nitrogen-stored materials for molecular studies at regular intervals; and e) natural course of disease with only symptomatic therapy (no specific anti-HIV treatment). It should be noted that at the final stage (year 5), due to the excessive loss of CD4 cells, recurrent infections by opportunists and additional pathologic changes (*e.g.* Kaposi's sarcoma) may have affected these patients. Therefore the data of year 5 may not reflect well the major features of HIV-1 infection alone and thus be excluded from the present study.

Peripheral blood lymphocytes of these 19 patients were typed by FITC-labeled monoclonal antisera using the diagnostic Ortho Spectrum III flow cytometer (Ortho Diagnostics, Neckargemuend, Germany). Antisera (Orthomue and Becton-Dickinson) were selected to identify mature T lymphocytes (CD3), thymic medullary lymphocytes CD4+8+, early thymic subcortical lymphocytes (CD38), stem cells (CD34), peripheral T helper cells (CD4) and cytotoxic T cells (CD8). Virus load was determined by the one-tube quantitative HIV-1 RNA NASBA amplification assay according to van Gemen *et al.* (1994) using the NASBA kit Nuclisens HIV-1 QT (Organon Teknika, Boxtel, The Netherlands) after RNA extraction from 1 ml of plasma. Plasma samples from the original studies were stored in liquid nitrogen until further use.

Table I summarizes the data as used in this paper. They actually represent the mean values of the 19 patients and serve as standard for validating our computational model. The virus load *(V*)* in terms of RNA copies ($\log_{10}/ml$) represent total concentrations of virus in plasma. At time 0 the virus load $V^*(0)$ is below the detectable threshold and thus unavailable. Its actual value will be estimated by our optimization algorithms later. The data of the CD38 cell counts ($z^*=Z^*/Z_0$), CD4 cell counts ($x^*=T^*/T_0$) and CD8 cell counts ($y^*=Y^*/Y_0$) are given as the relative values with

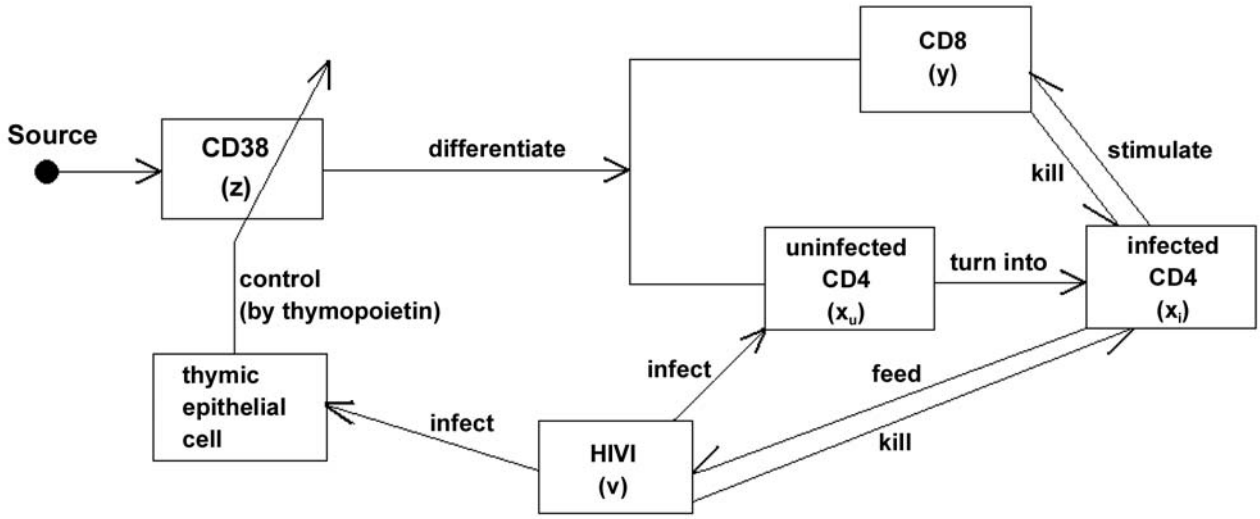

Figure 2. *The block diagram of the immunological network of HIV-1 infection.*

respect to the values of the age-matched healthy individuals, which are standard laboratory data established at the Immunopathology Laboratory, The University of Cologne, Germany (Habermann, 1991): $Z_0=80/\mu l$ for CD38 cell, $T_0=1000/\mu l$ for CD4 cell, and $Y_0=550/\mu l$ for CD8 cell. For example, $z^*(0)=2$ means that the CD38 value at the time of admission was about $160/\mu l$ (twice as the baseline value 80); $x^*(3)=0.333$ means that the CD4 value at year 3 was about $333/\mu l$ (one-third as the baseline value 1000).

Modeling

Tables II and III summarize all the variables and parameters used in the mathematical model.

Basic model (for the healthy people without virus infection). T cell counts remain fairly constant throughout the life of a healthy individual reflecting the internal balance between cell death and cell regeneration. This feature of the immune system is called homeostasis and can be modeled as

$$Z=S_Z-\delta_Z\cdot Z$$
$$T=A\cdot Z-\delta_T\cdot T$$
$$Y=B\cdot Z-\delta_Y\cdot Y \qquad \textbf{(1)}$$

Note that in the second and the third Equations the sources are proportional to Z, which embodies the fact that both CD4 T cells and CD8 T cells have differentiated from CD38 T cells.

In a state of health (no viral infection), cell counts are in homeostasis,

$$Z=T=Y=0 \qquad \textbf{(2)}$$

and possess constant values

$$Z=Z_0,\ T=T_0,\ \text{and}\ Y=Y_0. \qquad \textbf{(3)}$$

Table I. *Clinical data of HIV-1 virus load, CD38 cell (relative values), CD4 cell (relative values) and CD8 cell (relative values), during 4-years course of progressive infection.*

years		0	0.5	1	2	3	4
virus V^*			4.8	1.9	3.1	4.5	6.8
cell	CD38 z^*	2	3	2.5	2.8	4	6
counts	CD4 t^*	2	0.5	2	2	0.333	0.125
	CD8 y^*	2	3.9	3	3.1	2.7	2.7

Table II. *Variable details of the model.*

Variables	Definition	Units
Z	D38 cell counts	$/\mu l$
T	Uninfected CD4 cell counts	$/\mu l$
T_i	Infected CD4 cell counts	$/\mu l$
Y	CD8 cell counts	$/\mu l$
V	HIV-1 RNA copies	$\log_{10}$/ml

Substitute Eq. **(1)** by Eqs. **(2-3)**, one obtains $S_z=Z_0\delta_z$, $A=T_0\delta_T/Z_0$, and $B=Y_0\delta_Y/Z_0$.

Therefore Eq. **(1)** can also be expressed as

$$\dot{Z}=\delta_z\ (Z_0-Z)$$
$$\dot{T}=\delta_T\left(\frac{T_0}{Z_0}Z-T\right)$$
$$\dot{Y}=\delta_Y\left(\frac{Y_0}{Z_0}Z-Y\right) \qquad \textbf{(4)}$$

Table III. *Parameter details of the model.*

Parameters	Defination	Value	Units
Z_0	Baseline value of CD38 cells	80	/μl
T_0	Baseline value of CD4 cells	1000	/μl
Y_0	Baseline value of CD8 cells	550	/μl
$Z(0)$	Initial value of CD38 cells	204	/μl
$T(0)$	Initial value of uninfected CD4 cells	1811	/μl
$T_i(0)$	Initial value of infected CD4 cells	1.291	/μl
$Y(0)$	Initial value of CD8 cells	1721.5	/μl
$V(0)$	Initial value of virus load	0.10214	$\log_{10}$/ml
A	Source rate of CD4 cells	2.919	year^{-1}
B	Source rate of CD8 cells	0.58	year^{-1}
δ_Z	Diminishing (differentiation+death) rate of CD38 cells	2.1664	year^{-1}
δ_T	Death rate of the uninfected CD4 cells	1.7512	year^{-1}
δ_Y	Death rate of CD8 cells	0.69599	year^{-1}
β	Infection rate of T cells with free virus	5.84x10^{-4}	($\log_{10}$/ml)$^{-1}$year^{-1}
e	Death rate of the infected CD4 cells due to viral replication	9.9x10^{-5}	($\log_{10}$/ml)$^{-1}$year^{-1}
k	Death rate of the infected CD4 cells due to immune response	8.9832x10^{-3}	μl/year
g	Proliferation rate of CD8 cells due to viral stimulation	2.3047	μl/year
p	Virus production rate of infected CD4 cells	242.53	μl($\log_{10}$/ml)/year
c	Virion clearance rate	5.0x10^{-3}	μl/year
γ	Strength coefficient of the differentiation blockade effect	0.64635	(log10/ml)$^{-1}$
τ	Time lag between infection and death for CD4 cells	0.16846	year

Extended model for virus infection. The dynamics of cell infection and virion production is given by the following set of delay-differential equations (DDEs), which is a natural extention of Eq. **(4)**.

$$\dot{Z}=\delta_z\ (Z_0-f(V)\cdot Z)$$

$$\dot{T}=\delta_T\left(\frac{T_0}{Z_0}f(V)\cdot Z-T\right)-\beta VT$$

$$\dot{T}_i=\beta VT-eV(t-\tau)T(t-\tau)-kYT_i$$

$$\dot{Y}=\delta_Y\left(\frac{Y_0}{Z_0}f(V)Z-Y\right)+gT_iY$$

$$\dot{V}=pT_i-cYV \qquad \textbf{(5)}$$

The parameter explanation is as follows.

βVT represents virus infects healthy CD4 T cells. They appear in both the second and the third equations of system **(5)** with different signs.

$eV(t\text{-}\tau)T(t\text{-}\tau)$ represents the infected CD4 cells die in response to the virus replication (virus uses the resource of CD4 cells to replicate), where $\tau=\tau_1+\tau_2$. τ_1 represents the mean latent time of a virus life-cycle (virus production is assumed to lag by a discrete delay τ_1 behind the infection of a cell) (Herz, 1996; Culshaw & Ruan, 2000). τ_2 is the mean time between virus production and cell death. This implies that death rate of virus producing cells at time t is not given by the density of infected cells, but rather by the density of cells that were newly infected at time t-τ.

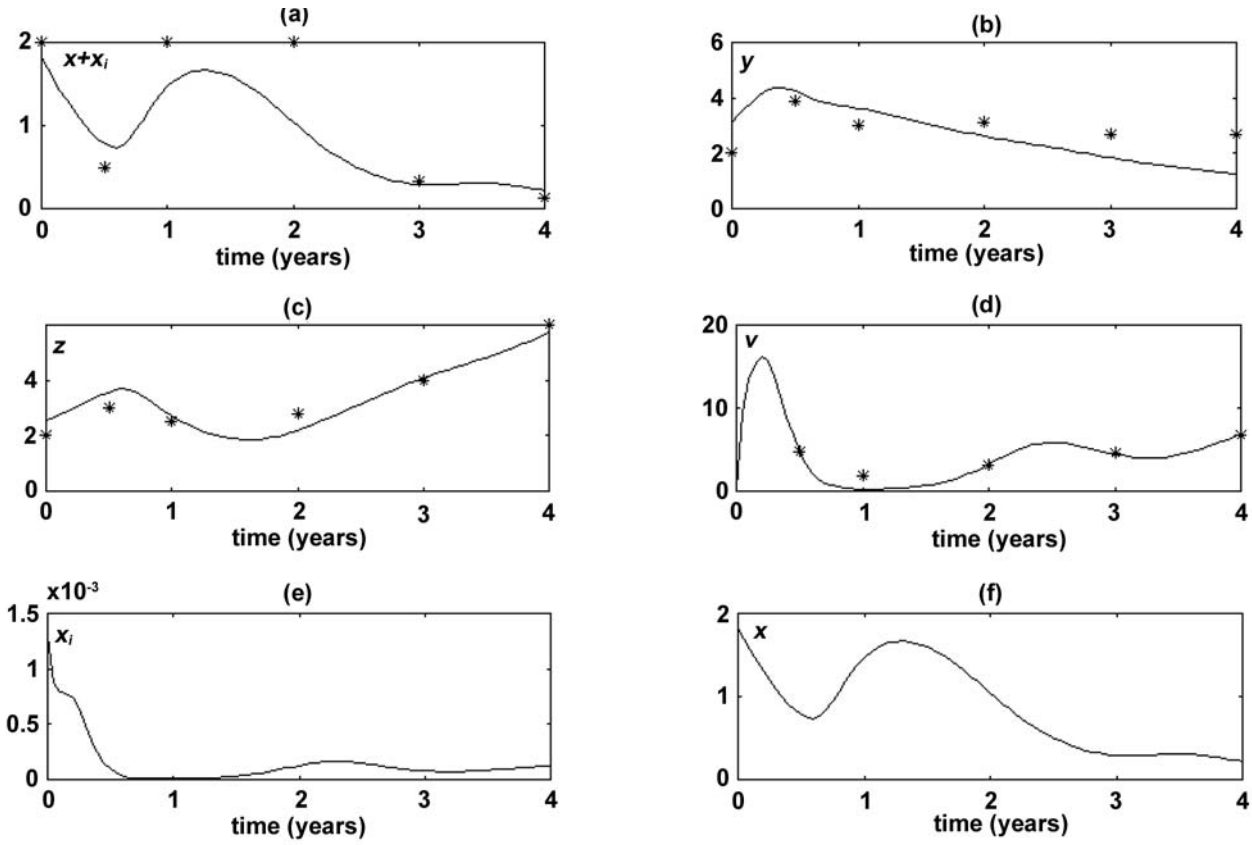

Figure 3. *Four-year simulation run with model (8) and parameter $P^{\#}$. z, x, x_i and y show the relative changes of CD38 cell, uninfected CD4 cell, infected CD4 cell and CD8 cell counts. V show changes of virus load. Stars represent the clinical data.*

kYT_i represents the infected CD4 cells die in response to the immune response by CD8 T cells.

gT_iY represents the infected CD4 cells antigenically stimulate the proliferation of CD8 cells. The virus proteins produced by a CD4 cell are cut into pieces and presented as peptide-MHC1 complex on the surface of that cell. CD8 cells with the correct T cell receptor will bind to the complex and in response begin to proliferate.

pT_i represents infected CD4 cells produce free virus particles.

cYV represents virion clearance. It is the result of immune elimination, or nonspecific remove by the reticuloendothelial system. At first we assumed it to be cV, but could not find any good simulation results. This may be because the fact only free (extracellular) virions can be cleared, while V also includes virions inside the CD4 cells. It is reasonable to assume that the percentage of free virions is proportional to Y, since the more immune CD8 cells affect virus containing cells, the greater the lytic bursts of infected CD4 cells, and the more virions are set free.

$f(V)$ appears before each Z-term in Eq. (**5**) and represents a differentiation blockade effect of the virus. It should be a decreasing function with

$$f(0)=1$$
$$f(\infty)=0 \qquad \textbf{(6)}$$

As V increases, $f(V)$ decreases. This also decreases the differentiation rate of CD38 cells while continuing to proliferate, due to the unaffected source rate. $\exp(-\gamma V)$ is a good candidate for $f(V)$ since it is a decreasing function satisfying Eq. (**6**). We use it and leave γ as a parameter to be determined in the next section.

It should be stressed that model (**5**) may also be applicable to other viruses with the same infection principle (targeting CD4 cells), such as the human herpesvirus-6 virus (HHV-6) (Krueger *et al.*, 1991a, b; Horwitz & Krueger, 1992), the human T cell leukemia virus type 1 (HTLV-1) (Copeland *et al.*, 1994; Brauweiler *et al.*, 1997). Therefore, some analytic results presented in the later part of this paper may also be applicable to these viruses. In the present paper, however, we only focus on HIV-1 data to validate the model, while other viruses may afford another set of parameters for model (**5**) with different outcomes respectively.

Parameter Optimization

Since the clinical data are given as relative values, for parameter optimization it is more convenient to use a "relative model" whose variables are relative values of T cell counts. By defining

$z(t)=Z(t)/Z_0$, $x(t)=T(t)/T_0$, $x_i(t)=T_i(t)/T_0$, $y(t)=Y(t)/Y_0$, **(7)**

model (5) is converted to a "relative" model as follows.

$z=\delta_z\ (1-\exp(-\gamma\cdot V)\cdot z)$

$x=\delta_t\ (\exp(-\gamma\cdot V)\cdot z-x)-\beta Vx$

$x_i=\beta Vx-eV(t-\tau)x(t-\tau)-k'yx_i$

$y=\delta_y\ (\exp(-\gamma\cdot V)\cdot z-y)+g'x_iy$

$V=p'x_i-c'yV$ **(8)**

where

$k'=kY_0$, $g'=gT_0$, $p'=pT_0$, $c'=cY_0$. **(9)**

There are a total of 16 parameters that need to be determined. They are: $z(0)$, $x(0)$, $x_i(0)$, $y(0)$, $V(0)$, δ_Z, δ_T, δ_Y, β, e, k', g', p', c', γ, τ. This is a difficult task considering the computational complexity. If one uses a brute force search and for every parameter checks N points, the total number for trial would be N^{16}, which is an astronomical number and far beyond the capability of present day computers even with N as small as 10.

In this paper, we use a direct search method (Lewis *et al.*, 1998 & 2000) that involves the minimization of an objective, defined in this paper as:

$$J(P)=\sum_{t=0.5,\ 1\text{-}4}\lambda_z(z(P,t)-z^*(t))^2+\sum_{t=0.5,\ 1\text{-}4}\lambda_x(x_i(P,t)+x(P,t)-x^*(t))^2$$

$$+\sum_{t=0.5,\ 1\text{-}4}\lambda_y(y(P,t)-y^*(t))^2+\sum_{t=0.5,\ 1\text{-}4}\lambda_v(V(P,t)-V^*(t))^2 \quad \textbf{(10)}$$

where

$P=(P_1, P_2, ..., P_{16})=(z(0), x(0), x_i(0), y(0), V(0), \delta_Z, \delta_T, \delta_Y, \beta, e, k', g', p', c', \gamma, \tau)$ is the set of parameters to be determined. Constraints to the parameters are:

1. $p>0$,
2. $V(0)\leq 1.9$ ($V(0)$ must be smaller than the detectable threshold, while 1.9 is the minimum of virus data and thus larger than the threshold).
3. $x_i(0)<0.01$ (In HIV-1 infection, only a small portion of PBL CD4 cells is infected (Abbas *et al.*, 2000)).

$z(P,t)$, $x(P,t)$, $xi(P,t)$ and $V(P,t)$ constitutes one simulation run generated by Eq. **(8)** under the parameter set P. λ_z, λ_x, λ_y and λ_V are weights to balance the objective. They are needed since z^*, x^*, y^* and V^* are in different order of magnitudes. We set $\lambda_\theta=1/(\theta^*_{max})^2$ ($\theta=z, x, y$ or V), where θ^*_{max} is the maximum value of $\theta^*(t)$, namely $\lambda_z=0.028$, $\lambda_x=0.25$, $\lambda_y=0.104$ and $\lambda_V=0.022$.

The aim is to minimize the objective $J(P)$ by changing the sixteen parameters respectively. That is, we first increase P_1 by a value ΔP_1. If this action makes the objective be smaller, we keep doing this to the point when the objective turns over, which means P_1 is over enlarged. We then split ΔP_1 in half, and repeat the abovementioned procedure. By doing this we will reach the point that changing P_1 will no longer affect the objective much. We then in turn change P_2, P_3, ..., P_{16}. In this way, the objective will be minimized at least to its local minimal (Lewis *et al.*, 2000; Polak, 1971). The detailed procedure can be summarized as follows.

Step 1. Set $j=0$, $m=0.1$.

Step 2. Within the constraints arbitrarily choose initial values for the parameters, $P=(P_1, P_2, ..., P_{16})$ with which Eq. **(8)** is solved by the fourth order Runge-Kutta algorithm. $J(P)$ is obtained by Eq. **(10)**.

Step 3. $j\rightarrow j+1$, if j reaches 17, set $j=1$, $m=0.1$.

Step 4. Increase P_j by a value m, *i.e.*, $P'=(P_1,...,P_{j+m},...,P_{16})$. If P_j+m exceeds its boundary value, then force it to be the boundary value. Obtain $J(P')$ following the same procedure as Step 2.

Step 5. If $|J(P)-J(P')|<\varepsilon$ (a given small value), then $P\rightarrow P'$, and then go to Step 3. Otherwise go to Step 6.

Step 6. If $J(P)-J(P')>0$, then $P\rightarrow P'$, and then go to Step 4. Otherwise make $m\rightarrow -m/2$ (change direction and halve the step size), then go to Step 4.

Note that in Step 4 the constraints for the parameters are enforced. For example, when $P_5=1.88$, $m=0.1$, $P_5+m=1.98$ exceeds its boundary value 1.9. Therefore it is forced to be 1.9.

Steps 1-6 cannot guarantee the algorithm to converge to a global minimal. Indeed in the first several weeks we can only get results that are not satisfactory. To jump out of local minimal, we re-run the search algorithm from time to time, with different sets of values as the initial parameters. Finally we succeed in getting a good result with parameter values as follows,

$P^\#=(2.5527, 1.8105, 1.291\text{x}10^{-3}, 3.1300, 0.10214, 2.1664, 1.7512, 0.69599, 5.84\text{x}10^{-4}, 9.9\text{x}10^{-5}, 4.4916, 2.3047\text{x}10^{3}, 2.4253\text{x}10^{5}, 2.7265, 0.64635, 0.16846)$.

Note that $z(0)$, $x(0)$, $x_i(0)$, $y(0)$, k', g', p', c' should be converted to $Z(0)$, $T(0)$, $T_i(0)$, $Y(0)$, k, g, p, c according to Eqs. **(7)** and **(9)**. The final parameter set is thus

$P^*=(204.2, 1810.5, 1.291, 1721.5, 0.10214, 2.1664, 1.7512, 0.69599, 5.84\text{x}10^{-4}, 9.9\text{x}10^{-5}, 8.9832\text{x}10^{-3}, 2.3047, 242.53, 5.0\text{x}10^{-3}, 0.64635, 0.16846)$, which is also shown in Table III.

The simulation run under $P^\#$ in comparison with the clinical data is shown in Figure 3. One sees that during the first half year viral replication leads to viremia, during which very high numbers of HIV-1 particles are present in the patient's blood. The viremia drops to a low level then climbs up again. CD38 (CD4) cell is approximately in- (anti-) phase with the virus. CD8 cell rises up during the first half year and then drops slowly. Only a very small fraction of CD4 cell is infected at any one time. The mean value of x_i is 0.000148, which is very close to the observed value 0.0001 (Abbas *et al.*, 2000).

Stability Analysis

The ODE model

We first study the stability of the ODE model

$$z=\delta_z\,(1-\exp(-\gamma\cdot V)\cdot z)$$
$$x=\delta_t\,(\exp(-\gamma\cdot V)\cdot z-x)-\beta Vx$$
$$x_i=\beta Vx-eVx-k'yx_i$$
$$y=\delta_y\,(\exp(-\gamma\cdot V)\cdot z-y)+g'x_iy$$
$$V=p'x_i-c'yV \qquad \textbf{(11)}$$

which differs from the DDE model **(8)** only in that $\tau=0$. The steady state of **(11)** is denoted by $\bar{\Gamma}=(\bar{z},\bar{x},\bar{x}_i,\bar{y},\bar{V})$. The Jocobian matrix at $\bar{\Gamma}$ is given by

$$J=\begin{bmatrix} -\delta_z\exp(-\gamma\,.\,\bar{V}) & -\delta_T\exp(-\gamma\,.\,\bar{V}) & 0 & -\delta_Y\exp(-\gamma\,.\,\bar{V}) & 0 \\ 0 & -\delta_T-\beta\bar{V} & (\beta-e)\bar{V} & 0 & 0 \\ 0 & 0 & -k'\bar{y} & g'\bar{y} & p'\bar{y} \\ 0 & 0 & -k'\bar{x}_i & -\delta_Y+g'\bar{x}_i & -c'\bar{V} \\ \gamma\delta_z\bar{z}\exp(-\gamma\,.\,\bar{V}) & -\gamma\delta_T\bar{z}\exp(-\gamma\,.\,\bar{V})-\beta\bar{x} & (\beta-e)\bar{x} & -\gamma\delta_Y\bar{z}\exp(-\gamma\,.\,\bar{V}) & -c'\bar{y} \end{bmatrix} \qquad \textbf{(12)}$$

The Uninfected Steady State $\bar{\Gamma}_u$

The ODE model (11) obviously has an uninfected steady state

$$\bar{\Gamma}_u=(1,\,1,\,0,\,1,\,0) \qquad \textbf{(13)}$$

with Jacobian matrix

$$J_u=\begin{bmatrix} -\delta_Z & \delta_T & 0 & \delta_Y & 0 \\ 0 & -\delta_T & 0 & 0 & 0 \\ 0 & 0 & -k' & g' & p' \\ 0 & 0 & 0 & -\delta_Y & 0 \\ \gamma\delta_Z & -\gamma\delta_T-\beta & \beta-e & -\gamma\delta_Y & -c' \end{bmatrix} \qquad \textbf{(14)}$$

and characteristic equation

$$(\lambda+\delta_Z)(\lambda+\delta_T)(\lambda+\delta_Y)\big(\lambda^2+(k'+c')\lambda+k'c'-p'(\beta-e)\big)=0. \qquad \textbf{(15)}$$

The eigenvalues are: $\lambda_1=-\delta_Z$, $\lambda_2=-\delta_T$, $\lambda_3=-\delta_Y$,

$$\lambda_{4,5}=\frac{-(k'+c')\pm\sqrt{(k'+c')^2-4\big(k'c'-p'(\beta-e)\big)}}{2}.$$

One sees that when $p'<k'c'/(\beta\text{-}e)$, $\lambda_4<0$ and thus $\bar{\Gamma}_u$ is stable; when $p'>k'c'/(\beta\text{-}e)$, $\lambda_4>0$ and thus $\bar{\Gamma}_u$ is unstable. p' is thus a bifurcation value that determines the stability of $\bar{\Gamma}_u$. This corresponds to the biological fact that if the virus production rate exceeds a critical value, the health state of the person is unstable and even a very small infection will lead to an uncontrolled virus production; If the virus production rate is less than the critical value, the health state is stable and the person can recover himself (by the immune response) without any clinical treatment.

For the parameter set $P^{\#}$ (with $\tau=0$ instead of 0.16846), we have $p'=242530>k'c'/(\beta\text{-}e)$ (=25250) $\bar{\Gamma}_u$, is thus unstable.

The Infected Steady State $\bar{\Gamma}_i$

Eq. **(11)** may have other steady states besides $\bar{\Gamma}_u$. They are called the infected steady states ($\bar{\Gamma}_i$) since $\bar{V}\neq 0$. From

$$\delta_z\,(1-\exp(-\gamma\bar{V})\cdot\bar{z})=0$$
$$\delta_T\,(\exp(-\gamma\bar{V})\cdot\bar{z}-\bar{x})-\beta\bar{V}\,\bar{x}=0$$
$$(\beta-e)\bar{V}\,\bar{x}-k'\bar{y}\bar{x}_i=0$$
$$\delta_y\,(\exp(-\gamma\bar{V})\cdot\bar{z}-\bar{y})+g'\bar{x}_i\bar{y}=0$$
$$p'\bar{x}_i-c'\bar{y}\bar{V}=0 \qquad \textbf{(16)}$$

one obtains

$$\bar{z}=\exp(\gamma\bar{V}) \qquad \textbf{(17)}$$

$$\bar{x}=\frac{\delta_T}{\beta\bar{V}+\delta_T} \qquad \textbf{(18)}$$

$$\bar{x}_i=\sqrt{\frac{c'\delta_T\,(\beta-e)}{p'k'}}\;\frac{\bar{V}}{\sqrt{\beta\bar{V}+\delta_T}} \qquad \textbf{(19)}$$

$$\bar{y}=\sqrt{\frac{p'\delta_T\,(\beta-e)}{c'k'}}\;\frac{1}{\sqrt{\beta\bar{V}+\delta_T}} \qquad \textbf{(20)}$$

$$\delta_y(1-\bar{y})+g'\bar{x}_i\bar{y}=0 \qquad \textbf{(21)}$$

From Eqs. **(19-21)** one obtains

$$\left(\beta+\frac{g'(\beta-e)\delta_T}{k'\delta_Y}\right)^2\bar{V}^2+\left(2\beta\delta_T+\frac{2g'(\beta-e)\delta_T^2}{k'\delta_Y}-\frac{p'\beta(\beta-e)\delta_T}{k'c'}\right)\bar{V}+\left(1-\frac{p'(\beta-e)}{k'c'}\right)\delta_T^2=0 \qquad (22)$$

Substitute the corresponding values in $P^{\#}$ into Eq. **(22)**, $\bar{V}$ is obtained as $\bar{V}=5.8793$

Other values are obtained as: $\bar{z}=44.706$, $\bar{x}=0.99804$, $\bar{x}_i=2.04\text{x}10^{-4}$, $\bar{y}=3.09$. Therefore, The ODE model **(11)** with the parameter set $P^{\#}$ (with $\tau=0$ instead of 0.16846) has only one infected steady state

$$\bar{\Gamma}_i=(44.706,\,0.99804,\,2.04\text{x}10^{-4},\,3.09,\,5.8793)$$

It follows from matrix **(12)** that the Jacobian matrix at $\bar{\Gamma}_i$ is

$$J_i=\begin{bmatrix} -0.04846 & 0.03917 & 0 & 0.01557 & 0 \\ 0 & -1.7546 & 0.00284 & 0 & 0 \\ 0 & 0 & -13.877 & 7122.3 & 242526 \\ 0 & 0 & -0.00092 & -0.2252 & -16.03 \\ 1.4004 & -1.1319 & 0.000482 & -0.44985 & -8.42466 \end{bmatrix}$$

The eigenvalues of J_i are solved with Matlab function eig(.) and the results are as follows.

$\lambda_1=-23.7$, $\lambda_2=0.029$, $\lambda_3=0.4445$, $\lambda_{4,5}=-0.5515\text{x}5.5076\text{i}$.

Since there are positive eigenvalues, $\bar{\Gamma}_i$ is obviously unstable.

The DDE model

The delay time τ does not change the steady states (and their instabilities, if any) of a dynamical system (Culshaw &

Ruan, 2000). Therefore the DDE model (8) with parameter $P^{\#}$ has the same $\bar{\Gamma}_u$, $\bar{\Gamma}_i$ and they are all unstable.

Discussion

Many excellent publications are available on using different techniques of computational simulation to study functions of the immune system (*e.g.*, Nowak & May, 1991; Nowak & Bangham, 1996; Perelson *et al.*, 1993&1996; Culshaw & Ruan, 2000; Brandt & Chen, 2001; Bar-Or & Segel, 1998; Segel & Bar-Or, 1999; Bar-Or, 2000; Kam *et al.*, 2001; Forrest & Hofmeyr, 2000; Warrender *et al.*, 2001; Kirschner *et al.*, 2000). Most of them focus on specific functional aspects in antigen / antibody / T cell regulation. They are therefore different from our goal of having a model with which we can simulate various cell pool changes of the immune system during the entire infectious course.

Some important works (*e.g.*, Mehr & Perelson, 1997; Kirschner *et al.*, 1998) did consider various cell changes(thymocytes, CD4 cells, and CD8 cells). However, their models differ from ours in many ways. Kirschner *et al.* (1998) pointed out that HIV-1 infection of the thymus may impede regeneration of the peripheral CD4 T cells. It is true that thymocyte infection can explain the depletion of CD4 cells, however, it alone is difficult to explain the concomitant proliferation of CD38 cells. Our cause for looking at the CD38 cell comes from their apparent importance in lymphoma development as indicators of early thymic cortical cells. Since HIV infects and destroys thymic epithelial cells (Kirschner *et al.*, 1998; Schnittman, 1991), further differentiation of T cells will become blocked just at that stage of CD38 cells. From Figure 3 one sees that changes in the CD4 cell counts, CD38 cell counts and the virus load occur in parallel. The CD4 cell is approximately anti-phase with the virus but CD38 cell is approximately in-phase with the virus. At year 0.5 the CD4 cell has a local minimum but the CD38 cell has a local maximum. At the final stage, CD4 cell depletes but CD38 cell proliferates. The underlying mechanism for this phenomenon may well be a certain block of intrathymic T cell maturation following destruction of thymic epithelial cells, as discussed previously (Seemayer *et al.*, 1984; Purtilo *et al.*, 1985; Kendall, 1986; Bonyhadi *et al.*, 1993; Braun *et al.*, 1996; Haynes *et al.*, 1998; Krueger *et al.*, 2001a). The reason is obvious: Once the differentiation is blocked, the CD4 cell and the CD8 cell decrease, and the undifferentiated CD38 cell has no outlet and continues to proliferate. In the present study, the effect has been modeled as exp (-γV) that appears before all the Z-terms in Eq. **(5)**. The simulation run fits well with the clinical data, which supports the differentiation blockade postulation from the viewpoint of mathematical modeling. This has not been done by other modeling works.

Stability analysis reveals that model (5) with parameter P^* has one uninfected steady state ($\bar{\Gamma}_u$) and one infected state ($\bar{\Gamma}_i$), but both are unstable. The large virus production rate makes the HIV-1 infection a malignant one, the patient can hardly recover once infected, due to the unstable $\bar{\Gamma}_u$. The T cell counts then diverge from the baseline values, but cannot reach any other steady states (due to the instability of $\bar{\Gamma}_i$), which leads to the uncontrolled proliferation of the virus and CD38 T cells, the depletion of CD4 T cells, as Figure 3 suggests. In the later stage, CD4 cell loss will result in rather complex and individually variable defects in host defense and cell proliferation. The consequence of such defects are recurrent infections by opportunists and other agents and uncontrolled cell proliferation in the immune system and in other cells with ultimate death from infections or neoplasia (Krueger *et al.*, 1991a). This may involve other biological mechanisms that have not been included in model **(5)**.

The project is based on a hypothesis of immunologic dysregulation of lymphoma development as described in previous publications and recently updated in a review paper (Krueger *et al.*, 2001b). According to this concept, diseases such as malignant lymphomas, aplasias or autoimmune disorders result from a disturbed balance of factors regulating cell proliferation, cell differentiation / function, and physiological cell death (apoptosis). Predominance of cell proliferation factors will ultimately cause lymphomas, predominance of apoptosis factors will cause aplasia, and unbalanced differentiation factors may contribute to autoimmune disorders. Viruses infections cause different prototype reactions (hyperplastic, aplastic, neoplastic) and are therefore very suitable for testing the immunologic dysregulation hypothesis of lymphoma development. For example, HHV-6-induced infectious mononucleosis represents a self-limited lymphoproliferative disease; HIV-1 infection represents a steadily progressive disease leading to final T cell immune deficiency and to death of the incumbent. HTLV-1-induced adult T cell leukemia (ATL) is a good example for a dysregulative leukemogenesis. In the present paper, we report only on HIV-1 infection for validating the conceptional model of cell pool changes in aplasia, hyperplasia and neoplasia. Our HIV cases were intentionally selected which ran a progressive course within a given time and which were not yet treated by anti-retroviral substances, thus representing a natural course of HIV-1 infection. The present model with some modification may also be applicable to other viruses as mentioned above, since they all target on the same CD4 T cell population and their underlying biological mechanisms are very similar. Bifurcation analysis may play an important role in finding different parameter regions for different diseases, or same disease with different levels of malignance. For example, we expect that in the HHV-6-induced infectious mononucleosis p' would be smaller than $k'c'/(\beta-e)$, since it represents a self-limited lymphoproliferative disease and the uninfected steady

state should be stable. The model thus appears to be a useful basis for further simulating disturbances of the T cell immune system and thus to elucidate the pathogenesis of various diseases including malignant lymphomas. If further developed adequately, it may well serve future clinical applications for diagnosis and treatment design.

References

1 Abbas AK, Lichtman AH and Pober JS: Cellular and Molecular Immunology. Philadephia: W.B. Saunders Company, 2000.

2 Abramson S, Miller RG and Philips RA: The identification in adult bone marrow of pluripotent and restricted stem cells of the myeloid and lymphoid system. J Exp Med *145*: 1567-1579, 1977.

3 Allison JP: Structure, function and serology of the T-cell antigen complex. Ann Rev Immunol *5*: 503-540, 1987.

4 Atkins B, Mueller C, Okada CY, Reinert RA, Weissman IL and Spangrude GJ: Early events in T-cell maturation. Ann Rev Immunol *5*: 325-365, 1987.

5 Bar-Or RL and Segel LA: On the role of a possible dialogue between cytokine and TCR presentation mechanisms in the regulation of autoimmune disease. J Theor Biol *190*: 161-178, 1998.

6 Bar-Or RL: Feedback mechanisms between T helper cells and macrophages in the determination of the immune response. Math Biosc *163*: 35-58, 2000.

7 Becker J, Ulrich P, Kunze R, Gelderblom H, Langford A and Reichart P: Immunohistochemical detection of HIV structural proteins and distribution of T-lymphocytes and Langerhans cells in the oral mucosa of HIV infected patients. Virchows Arch [A] *412*: 413-419, 1988.

8 Bonyhadi ML, Rabin L and Salimi S: HIV induces thymus depletion *in vivo*. Nature *363*: 728-732, 1993.

9 Brandt ME and Chen G: Feedback control of a biodynamical model of HIV-1. IEEE Transaction on Biomedical Engineering *48*: 754-759, 2001.

10 Braun J, Valentin H, Nugyere MT, Ohayon H, Gounon P and Barresinoussi F: Productive and persistent infection of human thymic epithelial cells *in vitro* with HIV-1. Virology *225*: 413-418, 1996.

11 Brauweiler A, Garrus JE, Reed JC and Nyborg JK: Repression of Bax gene expression by HTLV-1 Tax protain: implications for suppression of apoptosis in virally infected cells. Virology *28*: 135-140, 1997.

12 Chappell MJ, Godfrey KR and Vajda S: Global identifiability of the parameters of nonlinear systems with specified inputs: a comparison of methods. Math Biosci *102*: 41, 1990.

13 Copeland KF, Haaksma AG, Goudsmit J, Krammer PH and Hooney JL: Inhibition of apoptosis in T cells expressing human T cell leukemia virus type I Tax. AIDS Res Hum Retroviruses *10*: 1259-1268, 1994.

14 Crouse DA, Jordan RK and Sharp JG: T-cell differentiation. *In*: Immunoglobulin Genes and Cell Differentiation (Battisto & Knight eds.): 65-78, Elsevier-North Holland, Amsterdam NL, 1980.

15 Culshaw RV and Ruan S: A delay-differential equation model of HIV infection of CD4+ T-cells. Math Biosci *165*: 27-39,2000.

16 Dappen GE, Crouse DA, Anderson RW, Jordan RK, Robinson JH and Sharp JG: Morphological assessment of immunologically relevant cells in the thymus. Adv Exp Biol Med *149*: 389-399, 1982.

17 Essunger P and Perelson AS: Modeling HIV infection of CD4+ T-cell subpopulations. J Theor Biol *170*: 367-391, 1994.

18 Evans ND, Chapman MJ, Chappell MJ and Godfrey KR: Identifiability of uncontrolled nonlinear rational systems. Automatica *38*: 1799-1805, 2002.

19 Fauci AS and Clifton H: Human immunodeficiency virus (HIV) disease: AIDS and related disorders. Harrison's Principles of Internal Medicine, 15th Edition: 1131-1135, McGraw-Hill: Philadelphia, 2001.

20 Forrest S and Hofmeyr SA: Immunology as information processing. *In*: Design Principles for Immune System & Other Distributed Autonomous Systems (Segel LA and Cohen IR eds): 361-387, Oxford Univ Press, 2000.

21 Habermann UA: Relationship between T- and B-lymphocyte populations in AIDS patients with persistent or reactivated virus infections. MD thesis at University of Cologne, Medical Faculty, Kleikamp GmbH, Cologne, Germany, 1991.

22 Haynes BF and Hale LP: The human thymus. A chimeric organ comprised of central and peripheral lymphoid components. Immunol Res *18*: 61-78, 1998.

23 Heine UI, Krueger GRF, Karpinski A, Munoz E and Krueger MB: Quantitative light and electron microscopic changes in thymic reticular epithelial cells during moloneyvirus induced lymphoma development. J Cancer Res Clin Oncol *106*: 102-111,1983.

24 Herz AVM, Bonhoeffer S, Anderson RM, May RM and Nowak MA: Viral dynamics *in vivo*: Limitations on estimates of intracellular delay and virus decay. Proc Natl Acad Sci USA *93*: 7247-7251, 1996.

25 Horwitz CA, Krueger GRF, Steeper TA and Bertram G: HHV-6 Induced Mononucleosis-like Illnesses. Human Herpesvirus-6: 159-174, Elsevier Sci Publ: Amsterdam, 1992.

26 Kam N Cohen IR and Harel D: The immune system as a reactive system: modeling T cell activation with statecharts. Proc Symposia Human-Centric Computing Languages and Environments: 15-22, IEEE Computer Society Press: Stresa Italy, 2001.

27 Kendall MD: AIDS and the thymus. Immunology Today *7*: 254, 1986.

28 Kirn E, Eidt S, Krueger GRF, Koch B, Becker R, Wassermann K, Schrappe M and Fischer R: Coincidence of changes in diffuse lymphocyte populations in blood, bronchus- and gut-associated tissues (BALT and GALT) of HIV-positive patients. AIDS Forschg (AIFO) *8*: 411-418, 1993.

29 Kirschner DE, Mehr R and Perelson AS: Role of thymus in pediatric HIV-1 infection. J AIDS *18*: 95-109, 1998.

30 Kirschner DE, Webb GF and Cloyd M: Model of HIV-1 disease progression based on virus-induced lymph node homing and homing-induced apoptosis of CD4+ lymphocytes. J AIDS *24*: 352-362, 2000.

31 Kronenberg M, Siu G, Hood LE and Shastri N: The molecular genetics of the T-cell antigen receptor and T-cell antigen recognition. Ann Rev Immunol *4*: 529-591, 1986.

32 Krueger GRF, Ramon A, Degenhardt S, Schrappe-Baecher M, Rasokat H, Koch B and Deninger J: Cellular immunologic parameters in HIV-positive patients with AIDS-related complex and intravenous immunoglobulin therapy. Vox Sang *59*: 30-37, 1990.

33 Krueger GRF, Ablashi DV, Lusso P and Josephs SF: Immunological dysregulation of lymph nodes in AIDS patients. Current Topics in Pathology, Reaction Patterns of the Lymph Node. Part 2 Reactions Associated with Neoplasia and Immune Deficient States *84(2)*: 157-188, 1991.

34 Krueger GRF, Ablashi DV, Josephs SF, Salahuddin SZ, Lembke U, Ramon A, Hoffmann A and Bertram G: Clinical indication and current techniques for the demonstration of infection with human herpesvirus-6 (HHV-6). In Vivo *5*: 287-296, 1991.

35 Krueger GRF, Brigitte K, Weldner JD, Tymister G, Ramon A, Brandt ME, Wang G and Buja LM: Dynamics of active progressive infection with HIV-1: data acquisition for computer modeling. In Vivo *15*: 513-518, 2001.
36 Krueger GRF, Nguyen A, Uthman M, Brandt ME and Buja LM: Dysregulative lymphoma theory revisited: what can we learn from cytokines, CD classes and genes? Anticancer Res *21*: 3653-3661, 2001.
37 Lewis RM, Torczon V and Trosset MW: Why pattern search works. Optima: 1-7, 1998.
38 Lewis RM, Torczon V and Trosset MW: Direct search method: then and now. J Comput Appl Math *124*: 191-207, 2000.
39 Ljung L and Glad T: On global identifiability for arbitrary model parametrizations. Automatica *30(2)*: 265, 1994.
40 Lobach DF and Haynes BF: Ontogeny of the human thymus during fetal development. J Clin Immunol *7*: 81-97, 1987.
41 Marrack P, Lo D and Brinster R: The effect of thymus environment on T-cell development and tolerance. Cell *53*: 627-634, 1988.
42 Mehr R and Perelson AS: Blind T-cell homeostasis and the CD4/CD8 ratio in the thymus and peripheral blood. J AIDS *14*: 387-398, 1997.
43 Miescher C, Howe RC, Budd RC and MacDonald HR: Expression of T-cell receptors by functionally distinct subsets of immature adult thymocytes. Ann NYAS *532*: 8-17, 1988.
44 Müller TG, Noykova N, Gyllenberg M and Timmer J: Parameter identification in dynamical models of anaerobic waste water treatment. Math Biosc *177,178*: 147-160, 2002.
45 Nowak MA and May RM: Mathematical biology of HIV infection: antigenic variation and diversity threshold. Math Biosci *106*: 1, 1991.
46 Nowak MA and Bangham RM: Population dynamics of immune responses to persistent viruses. Science *272*: 74, 1996.
47 Pauza CD: HIV persistence in monocytes leads to pathogenesis and AIDS Cell Immunol *112*: 414-424, 1988.
48 Peled A, Petit I and Kollet O: Dependence of human stem cell engraftment and repopulation of NOD/SCID mice on CXCR4. Science *283*: 845-848, 1999.
49 Perelson AS, Kirschner DE and De Boer R: Dynamics of HIV infection of CD4+ T-cells. Math Biosci *114*: 81, 1993.
50 Perelson AS, Neumann AU, Markowitz M, Leonard JM and Ho D: HIV-1 dynamics *in vivo*: virion clearance rate, infected cell life-span, and viral generation time. Science *271*: 1582-1586, 1996.
51 Polak E: Computational Methods in Optimization: A Unified Approach. Academic Press: New York, 1971.
52 Purtilo DT, Tatsumi E, Manolov G, Manolova Y, Harada S, Lipscomb H and Krueger GRF: Epstein-Barr virus as an etiologic agent in the pathogenesis of lymphoproliferative and aproliferative diseases in immune deficient patients. Int Rev Exp Path *27*: 113-183, 1985.
53 Rappersberger K, Gartner S and Schenk P: Langerhans' cells are an actual site of HIV-1 replication. Intervirology *29*: 185-194, 1988.
54 Redfield RR, Wright DC and Tramont EC: Special report: the Walter-Reed staging classification for HTLV/ALV infection. N Engl J Med *311*: 131-132, 1986.
55 Rothenberg E and Lugo JP: Differentiation and cell division in the mammalian thymus. Developmental Biol *112*: 1-17, 1985.
56 Seemayer TA, Laroche AG, Russo P, Malebranche R, Arnoux E, Guerin JM, Pierre G, Dupuy KM, Gartner JG, Lapp WJ, Spira TJ and Elie R: Precocious thymic involution manifested by epithelial injury in the acquired immune deficiency syndrome. Hum Path *15*: 469-474, 1984.
57 Segel LA and Bar-Or RL: On the role of feedback in promoting conflicting goals of the adaptive immune system. J Immunol *163*: 1342-1349, 1999.
58 Shnittman SM, Singer KH, Greenhouse JJ *et al*: Thymic microenvironment induces HIV infection: Physiologic secretion of IL-6 by thymic epithelial cells up-regulates virus expression in chronically infected cells. J Immunol *147*: 2553-2558, 1991.
59 Sinangil F, Loyter A and Volsky DJ: Quantitative measurement of fusion between human immunodeficiency virus and cultured cells using membrane fluorescence sequencing. FEBS Lett *239*: 88-92, 1988.
60 Stutman O: Intrathymic and extrathymic T-cell maturation. Immunol Rev *42*: 138-184, 1978.
61 Surh CD and Sprent J: The thymus and T-cell development. Chapter 9 in: Inflammation: Basic Principles and Clinical Correlates (Gallin JI *et al*, eds): 137-149, Lippincott Williams & Wilkins: Philadelphia, 1999.
62 Thiele J, Wickenhauser C and Baldus SE: Characterization of CD34+ human hematopoietic progenitor cells from the peripheral blood: enzyme-, carbohydrate- and immuno-cytochemistry, morphometry, and ultrastructure. Leukemia & Lymphoma *16*: 483-491, 1995.
63 Tymister G: Korrelation von lymphozytenpopulationen, klinischer symptomatik und verlauf bei patienten mit erworbener abwehrschwache (AIDS). MD thesis at University of Cologne: 1-149, Hundt Druck GmbH, Cologne, 1988.
64 Vajda S, Godfrey KR and Rabitz H: Similarity transformation approach to identifiability analysis of nonlinear compartmental models. Math Biosci *93*: 217-248, 1989.
65 van Gemen, B, van Beuningen, R, Nabbe, A, van Strijp, D, Jurriaans, S, Lens P and Kievits T: A one-tune quantitative HIV-1 RNA NASBA nucleic acid amplification assay using electrochemiluminescent (ECL) labelled probes. J Viol Methods *49*: 157-168, 1994.
66 Warrender C, Forrest S and Segel L: Effective feedback in the immune system. *In*: Genetic and Evolutionary Computation Conference Workshop Program (Morgan & Kaufmann, eds): 329-332, 2001.
67 Wognum AW, DeJong MO and Wagemaker G: Differential expression of receptors for hematopoietic growth factors on subsets of CD34+ hemopoietic cells. Leukemia & Lymphoma *24*: 11-25, 1996.

Received June 3, 2003
Accepted December 19, 2003